Probabilistic Aspects of Magnetization Relaxation in Single-Domain Nanomagnets

G. Bertotti, C. Serpico, and I. D. Mayergoyz

Probabilistic aspects of magnetization relaxation in single-domain nanomagnets

G. Bertotti,[1] C. Serpico,[2] I. D. Mayergoyz[3]

[1] *INRIM, Istituto Nazionale di Ricerca Metrologica, Strada delle Cacce 91, 10135 Torino, Italy*
[2] *Dip. di Ing. Elettrica, University of Napoli "Federico II", via Claudio 21, 80125 Napoli, Italy*
[3] *Dept. of Electr. and Computer Engineering, University of Maryland, College Park MD 20742*

A single-domain nanomagnet is a basic example of system where relaxation from high to low energy is probabilistic in nature even when thermal fluctuations are neglected. The reason is the presence of multiple stable states combined with extreme sensitivity to initial conditions. It is demonstrated that for this system the probability of relaxing from high energies to one of the stable magnetization orientations can be tuned to whatever desired value between 0 and 1 by applying a small transverse magnetic field of appropriate amplitude. In particular, exact analytical predictions are derived for the conditions under which the probability of reaching one of the stable states becomes exactly 0 or 1. Under these conditions, magnetization relaxation is totally insensitive to initial conditions and the final state can be predicted with certainty, a feature that could be exploited to devise novel magnetization switching strategies or novel methods for the measurement of the magnetization damping constant.

Single-domain nanomagnets occupy a central position in the research on magnetic phenomena and applications at sub-micrometer scales, like coherent magnetization switching [1–4], current-induced magnetic torques [5–8], nanomagnet logic [9]. Also, they are appealing systems for the study of the ultimate thermodynamic limits of computation, expressed by Landauer's principle [10–12].

Fundamental as well as application-oriented research in this field revolves around the central question: how can one drive a nanomagnet to a prescribed final magnetization state ? The simplest answer, which is to apply a sufficiently large magnetic field that destroys all magnetic energy minima except one, is at the core of the classical Stoner-Wohlfarth model [13]. However, this strategy is unsatisfactory in many respects, and the search for more advanced alternatives has become the key issue in recent years, in relation for example to precessional [14–16] or spin-torque-driven [8, 17, 18] magnetization switching.

A striking feature revealing that a general answer to the previous question is far from trivial is the fine interlacing of the basins of attraction of stable magnetization states under zero external field (Fig. 1(a)). This interlacing is the consequence of dissipative mechanisms which are a rather weak perturbation of constant-energy precessional dynamics. The result is an extreme sensitivity to initial conditions. As a consequence, a nanomagnet brought to an unstable initial state will relax to a final magnetization orientation which appears to be unpredictable, because control of initial conditions is always imperfect, due to thermal fluctuations or other disturbances [19].

In the language of dynamical system theory, the picture we are describing is that of a weakly dissipative system where multiple stable states exist and sensitivity to initial conditions introduces probabilistic aspects in an otherwise purely deterministic dynamics [20–23]. This problem is of very general nature [24, 25], and is encountered in many other fields of science, from stability of planetary motion in the solar system, to motion of charged particles in electric and magnetic fields, to propagation of electromagnetic waves (see [26] and references therein).

A central role is played in weakly dissipative systems by the notion of averaging and separatrix crossing [21–23]. The fact is that weak dissipation implies the existence of two distinct time scales: a fast scale on which motion at nearly constant energy takes place; and a slow scale on which energy decreases due to dissipation. The slow relaxation in energy, revealed by averaging over the fast scale, provides the core information about the behavior of the system. However, when the system can relax to multiple low-energy states the energy description becomes incomplete, because one needs additional information about which low-energy state is selected when the system crosses the saddle separatrix between high and low energy. This additional information is expressed in probabilistic terms, by introducing the notion of probability P_i of relaxation from high energies to one of the available stable states s_i.

In this Letter, we demonstrate that in a single-domain nanomagnet the relaxation probabilities P_i can be tuned to whatever desired value between 0 and 1 by applying a small transverse magnetic field. The field neither breaks the mirror symmetry of the energy function with respect to the final stable states nor introduces any important distortion in the energy profile. Nevertheless, the small energy term that is added to the dynamics is enough to alter the effect of the weak dissipative part in a way that drastically modifies the relaxation probabilities. In particular, one can achieve a complete restructuring of the basins of attraction, in which the probability of reaching one of the stable states becomes exactly 0 or 1 (Fig. 1(b)). Under these conditions, magnetization relaxation is totally insensitive to initial conditions and the
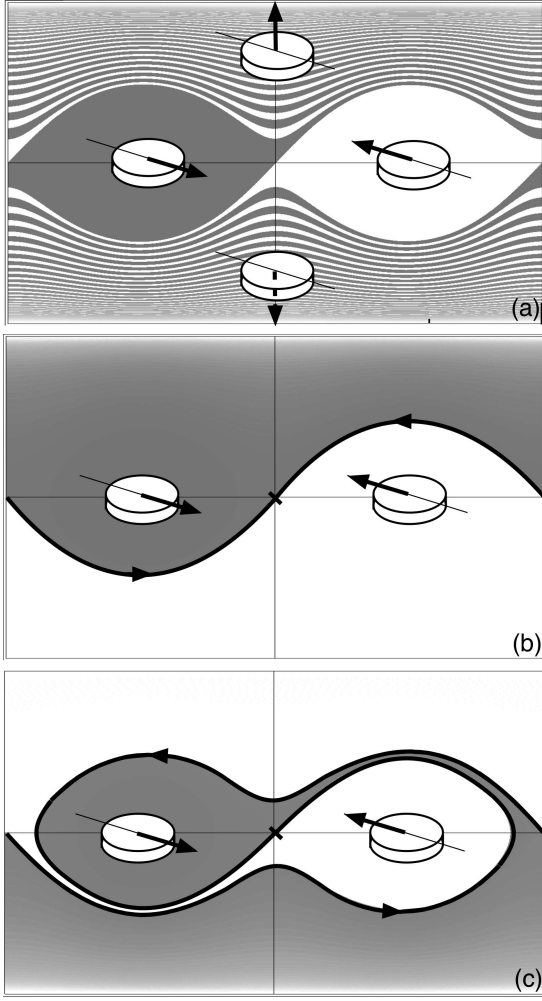
FIG. 1: Single-domain nanomagnet with easy, intermediate, and hard magnetic axes along $\mathbf{e}_x$, $\mathbf{e}_y$, and $\mathbf{e}_z$ directions, respectively. Figure shows numerically computed basins of attraction of $m_x > 0$ (gray) and $m_x < 0$ (white) stable states under transverse external field $h_a \mathbf{e}_y$. Representation is in (m_z, ϕ) plane. Abscissa: $-\pi/2 \leq \phi < 3\pi/2$. Ordinate: $-1 < m_z < 1$. (a): $h_a = 0$. (b): $h_a = 0.005477225$. (c): $h_a = 0.01635185$. Value in (b) coincides with $\alpha \sqrt{D_{zy} D_{yx}}$. Bold oriented lines represent saddle connections discussed in the text. Parameters: $D_{yx} = 0.3$, $D_{zy} = 1$, $\alpha = 0.01$.

final state can be predicted with certainty, a feature that could be exploited to devise novel magnetization switching strategies.

To start the technical discussion, consider a single-domain nanomagnet with total (i.e., crystal + shape) ellipsoidal anisotropy and principal axes along x, y, z. Assume that these axes represent the magnetic easy, intermediate, and hard axes, respectively. Then, the anisotropy coefficients are ordered in the following manner: $D_x < D_y < D_z$. For example, one has: $D_x < 0, D_y \sim 0, D_z \sim 1$ for a nanodot with in-plane anisotropy along x. In the subsequent discussion, we shall use the

quantities: $D_{yx} = D_y - D_x$, $D_{zy} = D_z - D_y$, which are both positive under the mentioned assumptions.

Assume that the nanomagnet is subjected to the external magnetic field $\mathbf{h}_a = h_a \mathbf{e}_y$ applied along the intermediate axis. Then the energy of the system is:

$$g(\mathbf{m}; h_a) - \frac{1}{2}D_y = \frac{1}{2}\left(D_{zy}m_z^2 - D_{yx}m_x^2\right) - h_a m_y \quad . \quad (1)$$

In this expression, the energy is written in dimensionless form, in units of $\mu_0 \mathrm{M}_s^2 V$, where V is the nanomagnet volume and M_s is the spontaneous magnetization. The vector $\mathbf{m}$ represents the normalized ($|\mathbf{m}|^2 = 1$) magnetization, while h_a is the dimensionless external field amplitude, measured in units of M_s. In subsequent expressions, we shall omit the inessential $D_y/2$ offset.

Our analysis is limited to the field interval $0 \leq h_a \leq D_{yx}$, in which the energy displays the following critical points:

- Two symmetric energy minima s_1 and s_2 in the regions $m_x > 0$ and $m_x < 0$, respectively.

- Two saddles d and d' at $m_x = 0$, $m_y = \pm 1$, $m_z = 0$, with energy $g_d = -h_a$, $g_{d'} = h_a$, respectively.

- Two energy maxima u_1 and u_2 in the regions $m_z > 0$ and $m_z < 0$, respectively.

When thermal fluctuations can be neglected, magnetization relaxation is governed by the deterministic Landau-Lifshitz (LL) equation [27], which is expressed in dimensionless form as:

$$\frac{d\mathbf{m}}{dt} = -\mathbf{m} \times \mathbf{h}_{\mathrm{eff}} - \alpha\,\mathbf{m} \times (\mathbf{m} \times \mathbf{h}_{\mathrm{eff}}) \quad . \quad (2)$$

In this equation, $\mathbf{h}_{\mathrm{eff}} = -\partial g/\partial \mathbf{m}$ is the effective field, α is the damping constant, and t is dimensionless time, measured in units of $(\gamma \mathrm{M}_s)^{-1}$ (γ is the absolute value of the gyromagnetic ratio). From Eq. (1) one finds that $\mathbf{h}_{\mathrm{eff}} = \mathbf{h}_M + h_a \mathbf{e}_y$, where:

$$\mathbf{h}_M = D_{yx}m_x\mathbf{e}_x - D_{zy}m_z\mathbf{e}_z \quad , \quad (3)$$

$\mathbf{e}_x$, $\mathbf{e}_y$, and $\mathbf{e}_z$ being unit vectors along the reference axes. When convenient, cylindrical $\mathbf{m}$ coordinates (m_z, ϕ) will be used, defined by the relations: $m_x = \sqrt{1 - m_z^2}\,\cos\phi$, $m_y = \sqrt{1 - m_z^2}\,\sin\phi$.

To understand the physical origin of the dramatic basin restructuring illustrated by Fig. 1, consider first the pure precessional dynamics under $\alpha = 0$ and $h_a = 0$:

$$\frac{d\mathbf{m}}{dt} = -\mathbf{m} \times \mathbf{h}_M \quad . \quad (4)$$
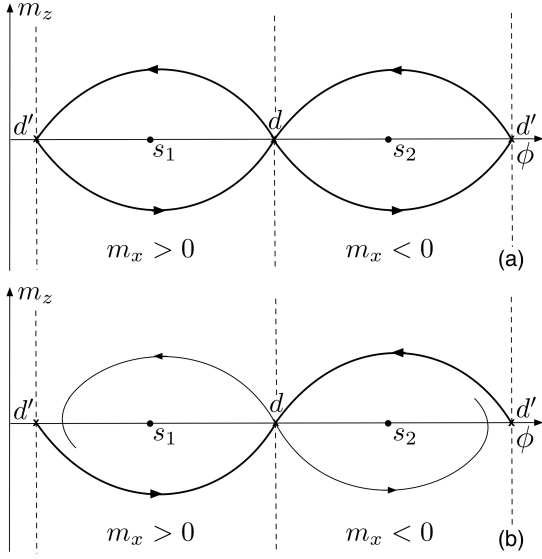
FIG. 2: Representation of magnetization dynamics in (m_z, ϕ) plane: $-\pi/2 \leq \phi < 3\pi/2$, $-1 < m_z < 1$. (a): Precessional dynamics under $\alpha = 0$ and $h_a = 0$. Oriented lines represent saddle-to-saddle connections. (b): Formation of saddle connections in dissipative dynamics at $h_a = \alpha \sqrt{D_{zy} D_{yx}}$ (compare with Fig. 1(b)).

This dynamics is dominated by the four saddle-to-saddle trajectories (heteroclinic saddle connections) shown in Fig. 2(a). These connections are curves of constant energy $g = 0$, which subdivide the (m_z, ϕ) plane into two low-energy regions around the energy minima s_1 and s_2 and two high-energy regions at $m_z > 0$ and $m_z < 0$, respectively.

The introduction of damping breaks all these connections, because energy decreases along any dissipative trajectory, and therefore it is no longer possible that a trajectory may connect saddles with identical energy $g_d = g_{d'} = 0$. However, if one also introduces the transverse field $h_a \mathbf{e}_y$, then the saddles acquire different energies ($g_d = -h_a$, $g_{d'} = h_a$), and a trajectory from saddle to saddle may be realized if the energy dissipated along the trajectory coincides with the saddle energy splitting. Indeed, when this is the case, two connections are simultaneously formed because of symmetry (Fig. 2(b)). When these dissipative connections are formed, they create an impenetrable barrier to magnetization dynamics. The result is that no trajectory originated from the vicinity of the energy maximum u_1 at $m_z > 0$ can reach s_2, and similarly no trajectory from the vicinity of u_2 can reach s_1. The phase portrait is reduced to fully separated basins of attraction, with no interlacing, and magnetization relaxation becomes totally insensitive to initial conditions (Fig. 1(b)).

The value of h_a at which the connections shown in Fig. 2(b) are formed under given damping α can be de-

termined by exploiting the following remarkable property of the dissipative dynamics, demonstrated below:

- the dissipative connections shown in Fig. 2(b) are *identical in geometric shape* to the two corresponding conservative connections present in Fig. 2(a).

In other words, the combined introduction of damping and external field distorts all the trajectories of the conservative dynamics (4), except for the two connections shown in Fig. 2(b), which remain unchanged if the field is properly tuned. It is important to stress that, although the shape of the connections remains the same, the magnetization variation along them is rescaled in time by a proper factor, also derived below.

To prove all this, consider, in Fig. 2(a), one of the two conservative connections for which m_x and m_z have opposite sign. The connection is a trajectory for which $h_a = 0$ and $g = 0$. Consequently, one obtains from Eq. (1) that it is characterized by the relation: $\sqrt{D_{yx}}\, m_x = -\sqrt{D_{zy}}\, m_z$. Use of this relation in Eq. (3) yields: $\mathbf{h}_M = \sqrt{D_{zy} D_{yx}}\, \mathbf{m}_{d'd}(t) \times \mathbf{e}_y$, where $\mathbf{m}_{d'd}(t)$ represents the solution of Eq. (4) associated with the connection.

Consider now the vector function $\mathbf{m}_{d'd}(rt)$, where r is a factor to be determined. The expression derived above for $\mathbf{h}_M$ is valid also for $\mathbf{m}_{d'd}(rt)$. Thus:

$$\mathbf{h}_M = Q\, \mathbf{m}_{d'd}(rt) \times \mathbf{e}_y \ , \ \ Q = \sqrt{D_{zy} D_{yx}} \ . \tag{5}$$

Furthermore, since $\mathbf{m}_{d'd}(t)$ satisfies Eq. (4), one has:

$$\frac{d}{dt}\mathbf{m}_{d'd}(rt) = -rQ\, \mathbf{m}_{d'd}(rt) \times \left[\mathbf{m}_{d'd}(rt) \times \mathbf{e}_y\right] \ , \tag{6}$$

where use has been made of Eq. (5). By substituting $\mathbf{m}_{d'd}(rt)$ for $\mathbf{m}$ in Eq. (2), by using Eqs. (5) and (6), and by taking into account that $\mathbf{h}_{eff} = \mathbf{h}_M + h_a \mathbf{e}_y$, one reduces Eq. (2) to the equation:

$$\left[rQ - (Q + \alpha h_a)\right] \mathbf{m}_{d'd} \times (\mathbf{m}_{d'd} \times \mathbf{e}_y)$$
$$- (h_a - \alpha Q)\, \mathbf{m}_{d'd} \times \mathbf{e}_y = 0 \ . \tag{7}$$

Inspection of Eq. (7) reveals that $\mathbf{m}_{d'd}(rt)$ is indeed a solution of the general LL equation provided:

$$h_a = \alpha Q \ , \ \ r = 1 + \alpha^2 \ . \tag{8}$$

The condition $h_a = \alpha Q$ for the formation of the saddle connection is exact for any value of damping. Since the saddle energy splitting is equal to $2h_a$, one concludes that $2\alpha Q$ represents the amount of energy dissipated in the magnetization motion along the connection.

Other conditions for the formation of saddle connections can be derived in the case when both α and h_a

are sufficiently small. Indeed, in this case any saddle-to-saddle trajectory will stay close to the zero-damping connections of Fig. 2(a). But there are multiple paths connecting d' to d by staying close to these connections. These paths consist of a first part $[d'd]$ from d' to the vicinity of d, followed by a certain number of almost closed loops $[dd'd]$ alternatively going around s_1 or s_2. The energy dissipation along these paths is quantized, because it is approximately equal to $2\alpha Q$ for the first $[d'd]$ part and then to $4\alpha Q$ for each of the subsequent $[dd'd]$ loops. Since the connection must connect two saddles whose energy difference is $2\,h_a$, the condition for the formation of a connection containing k $[dd'd]$ loops is $2h_a \simeq 2\alpha Q + 4k\alpha Q$. Hence, the set of critical fields at which saddle-to-saddle connections are realized under small α and h_a is:

$$h_k \simeq (2k+1)\,\alpha Q \ , \ \ k = 0, 1, 2, \ldots \ . \tag{9}$$

The first critical field h_0 coincides with the field in Eq. (8). This field is of the order of 1 mT in a system for which $\mu_0 M_s \sim 1$ T, $\alpha \sim 0.01$, $Q \sim 0.1$. Figures 1(b) and 1(c) show the basin structure existing at the critical fields h_0 and h_1, respectively.

Basin restructuring was tested by numerically integrating the LL equation for a large number ($\sim 10^6$) of initial conditions distributed at random in the high-energy region with $m_z > 0$. The integration was repeatedly carried out under progressively increasing values of the external field h_a. The number of trajectories reaching the s_2 energy minimum always dropped down to exactly zero when the condition $h_a = \alpha \sqrt{D_{zy}D_{yx}}$ was reached. It was also numerically checked that the same effect periodically appeared under further increase of the external field (Fig. 1(c)). The corresponding numerical estimate for the critical field h_1 (see figure caption) is within 1% from the prediction of Eq. (9).

One can represent the sequence (9) by straight lines in the plane (h_a, α) (Fig. 3(a)). Along each line, the probability of reaching s_1 starting from high-energy initial conditions with $m_z > 0$ is either 1 or 0. Figure 3 has important implications. Indeed, in the literature on weakly dissipative systems the probability P_i of relaxation to the stable state s_i is mathematically defined by the following double, non-interchangeable limit [22]:

$$P_i = \lim_{D \to 0} \lim_{\alpha \to 0} \frac{n_i}{n} \ , \tag{10}$$

where n_i/n represents the fraction of states that relax to s_i starting from high-energy initial conditions within a certain distance D from a given state u. The definition (10) is obviously based on the assumption that the limit of n_i/n for $\alpha \to 0$ does exist. In other words, one assumes that the only effect of a decrease in dissipation is that the fast and slow time scales get more and more separated,
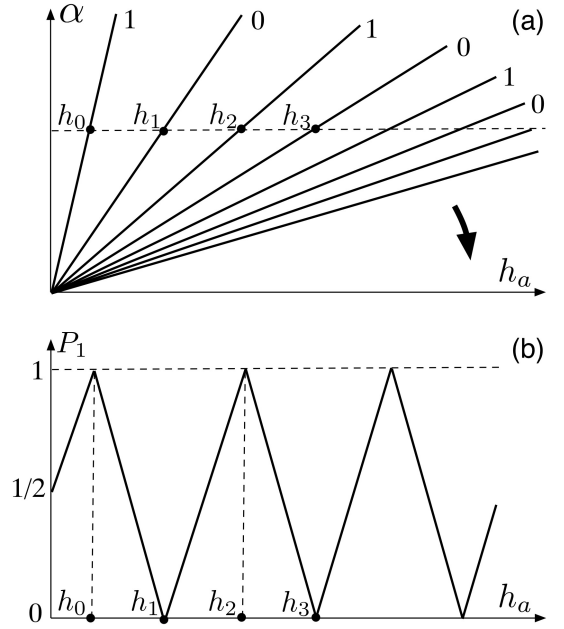

FIG. 3: (a): Family of critical lines (9) in (h_a, α) plane. Digits 1 and 0 represent the value of P_1 along the critical line. The arrow indicates the presence of additional critical lines, not shown in the figure, down to zero slope. (b): Corresponding behavior of P_1 as a function of h_a under constant α.

but that otherwise no qualitative change takes place in the dynamics. Figure 3(a) shows that this assumption cannot be made for the problem under discussion. Given the external field h_a, the probability P_1 indefinitely oscillates between 0 and 1 when $\alpha \to 0$, since all the critical lines of the family (9) are progressively crossed, and no limit exists.

As will be discussed in detail in a more extended paper under preparation, the notion of limiting probability of relaxation to one of the magnetization energy minima can be restored by a phase-flow description of magnetization relaxation. In this framework, the probability P_1 is defined in the joint limit ($\alpha \to 0, h_a \to 0$) under constant ratio $R = h_a/\alpha$. The phase-flow analysis predicts that P_1 will exhibit a piecewise linear dependence on R, reaching its extremum values, 0 or 1, in correspondence of the critical conditions (9) (Fig. 3(b)). Also this prediction was tested and confirmed by computer simulations.

There exists a direct connection between the methods discussed in this Letter and spin-transfer-driven magnetization dynamics. Indeed, the time-rescaled saddle-to-saddle trajectory $\mathbf{m}_{d'd}(rt)$ remains an exact solution even when one includes in Eq. (2) a spin-transfer torque $\beta\,\mathbf{m} \times (\mathbf{m} \times \mathbf{e}_y)$, carried by a current β of electrons with spin polarisation along $\mathbf{e}_y$. One can verify that the condition for the formation of the connection is still $h_a = \alpha Q$, and is therefore unaffected by the presence of the current. The current affects the time-rescaling factor r, which in

this case is equal to:

$$r = 1 + \alpha^2 - \beta/Q \ . \qquad (11)$$

This reveals that one can slow down the motion along the saddle connection to arbitrarily low rates by properly tuning the spin-polarized current density.

One expects that thermal fluctuations will mask the phenomena discussed in this Letter when the thermal energy $k_B T$ becomes comparable with the characteristic saddle energy splitting $2\alpha Q$. The condition for the observability of basin restructuring is therefore: $k_B T \ll 2\alpha Q \mu_0 M_s^2 V$. This yields $T \ll 10^2$ K for a nanodot with $V \sim 10^{-24}$ m^3, $\mu_0 M_s \sim 1$ T, $\alpha \sim 10^{-2}$, $Q \sim 0.1$. Thus, experiments at cryogenic temperatures should fully reveal basin restructuring phenomena. In particular, one should be able to measure α by means of experiments probing relaxation probabilities in arrays of weakly interacting nanodots brought close to the critical condition $h_a = \alpha Q$. This measurement of the damping constant would be related to the far-from-equilibrium dynamics of the nanodots at energies close to the saddle energy, quite differently from the conditions realized in quasi-equilibrium measurement methods [28].

---

[1] W. Wernsdorfer, E. B. Orozco, K. Hasselbach, A. Benoit, B. Barbara, N. Demoncy, A. Loiseau, H. Pascard, and D. Mailly, Phys. Rev. Lett. **78**, 1791 (1997).

[2] M. Bauer, J. Fassbender, B. Hillebrands, and R. L. Stamps, Phys. Rev. B **61**, 3410 (2000).

[3] Y. Acremann, C. H. Back, M. Buess, D. Pescia, and V. Pokrovsky, Appl. Phys. Lett. **79**, 2228 (2001).

[4] Z. Z. Sun and X. R. Wang, Phys. Rev. Lett. **97**, 077205 (2006).

[5] G. Bertotti, C. Serpico, I. D. Mayergoyz, A. Magni, M. d'Aquino, and R. Bonin, Phys. Rev. Lett. **94**, 127206 (2005).

[6] J. C. Sankey, Y. T. Cui, J. Z. Sun, J. C. Slonczewski, R. A. Buhrman, and D. C. Ralph, Nature Phys. **4**, 67 (2008).

[7] D. Li, Y. Zhou, B. Hu, and C. Zhou, Phys. Rev. B **84**, 104414 (2011).

[8] A. Brataas, A. D. Kent, and H. Ohno, Nature Mater. **11**, 372 (2012).

[9] M. T. Niemier, G. H. Bernstein, G. Csaba, A. Dingler, X. S. Hu, S. Kurtz, S. Liu, J. Nahas, W. Porod, M. Siddiq, et al., J. Phys.: Condens. Matter **23**, 493202 (2011).

[10] R. Landauer, IBM J. Res. Develop. **5**, 183 (1961).

[11] B. Lambson, D. Carlton, and J. Bokor, Phys. Rev. Lett. **107**, 010604 (2011).

[12] A. Berut, A. Arakelyan, A. Petrosyan, S. Ciliberto, R. Dillenschneider, and E. Lutz, Nature **483**, 187 (2012).

[13] E. C. Stoner and E. P. Wohlfarth, Phil. Trans. Roy. Soc. A **240**, 599 (1948).

[14] S. Kaka and S. E. Russek, Appl. Phys. Lett. **80**, 2958 (2002).

[15] G. Bertotti, I. D. Mayergoyz, C. Serpico, and M. d'Aquino, IEEE Trans. Magn. **39**, 2501 (2003).

[16] H. W. Schumacher, C. Chappert, R. C. Sousa, P. P. Freitas, and J. Miltat, Phys. Rev. Lett. **90**, 017204 (2003).

[17] Y. B. Bazaliy, B. A. Jones, and S. C. Zhang, Phys. Rev. B **69**, 094421 (2004).

[18] I. N. Krivorotov, N. C. Emley, J. C. Sankey, S. I. Kiselev, D. C. Ralph, and R. A. Buhrman, Science **307**, 228 (2005).

[19] C. Serpico, M. d'Aquino, G. Bertotti, and I. D. Mayergoyz, IEEE Trans. Magn. **45**, 5224 (2009).

[20] R. Haberman and R. Rand, Int. J. Nonlinear Mech. **34**, 1047 (1999).

[21] M. Brin and M. I. Freidlin, Ergodic Theory Dyn. Syst. **20**, 55 (2000).

[22] V. I. Arnold, V. V. Kozlov, and A. I. Neishtadt, *Mathematical Aspects of Classical and Celestial Mechanics* (Springer, Berlin, 2006).

[23] M. I. Freidlin and W. Hu, J. Stat. Phys **144**, 978 (2011).

[24] A. H. Nayfeh and D. T. Mook, *Nonlinear Oscillations* (Wiley Interscience, New York, 1979).

[25] J. Guckenheimer and P. Holmes, *Nonlinear Oscillations, Dynamical Systems, and Bifurcations of Vector Fields* (Springer, New York, 1997).

[26] A. I. Neishtadt, Chaos **1**, 42 (1991).

[27] G. Bertotti, I. D. Mayergoyz, and C. Serpico, *Nonlinear Magnetization Dynamics in Nanosystems* (Elsevier, Oxford, 2009).

[28] N. Liebing, S. Serrano-Guisan, A. Caprile, E. S. Olivetti, F. Celegato, M. Pasquale, A. Mueller, and H. W. Schumacher, IEEE Trans. Magn. **47**, 2502 (2011).